JOURNAL OF SOLID STATE CHEMISTRY 58, 257–266 (1985)

Nonstoichiometry and Defect Structure of the Perovskite-Type Oxides $La_{1-x}Sr_xFeO_{3-\delta}$

JUNICHIRO MIZUSAKI,* MASAFUMI YOSHIHIRO, SHIGERU YAMAUCHI, AND KAZUO FUEKI

Department of Industrial Chemistry, Faculty of Engineering, University of Tokyo, Hongo, Bunkyo-ku, Tokyo 113, Japan

Received April 23, 1984; in revised form December 10, 1984

In order to elucidate the defect structure of the perovskite-type oxide solid solution $La_{1-x}Sr_xFeO_{3-\delta}$ (x = 0.0, 0.1, 0.25, 0.4, and 0.6), the nonstoichiometry, δ, was measured as a function of oxygen partial pressure, P_{O_2}, at temperatures up to 1200°C by means of the thermogravimetric method. Below 200°C and in an atmosphere of $P_{O_2} \geq 0.13$ atm, δ in $La_{1-x}Sr_xFeO_{3-\delta}$ was found to be close to 0. With decreasing log P_{O_2}, δ increased and asymptotically reached $x/2$. The log(P_{O_2}/atm) value corresponding to $\delta = x/2$ was about -10 at 1000°C. With further decrease in log P_{O_2}, δ slightly increased. For $LaFeO_{3-\delta}$, the observed δ values were as small as <0.015. It was found that the relation between δ and log P_{O_2} is interpreted on the basis of the defect equilibrium among Sr'_{La} (or V'''_{La} for the case of $LaFeO_{3-\delta}$), $V_O^{\cdot\cdot}$, Fe'_{Fe}, and $Fe^{\cdot}_{Fe}$. Calculations were made for the equilibrium constants K_{ox} of the reaction

$$\tfrac{1}{2}O_2(g) + V_O^{\cdot\cdot} + 2Fe^{x}_{Fe} = O^{x}_{O} + 2Fe^{\cdot}_{Fe}$$

and K_i for the reaction

$$2Fe^{x}_{Fe} = Fe'_{Fe} + Fe^{\cdot}_{Fe}.$$

Using these constants, the defect concentrations were calculated as functions of P_{O_2}, temperature, and composition x. The present results are discussed with respect to previously reported results of conductivity measurements.

1. Introduction

Recently, much interest has been focused on the perovskite-type oxide solid solutions $La_{1-x}Sr_xMO_{3-\delta}$ (M = 3d transition metals such as Cr, Mn, Fe, Co, etc.), because these materials have high electronic and ionic conductivities and some show high catalytic activity. Many studies have been made to utilize these materials as catalysts, chemical sensor elements, electrodes for MHD generators and solid electrolyte fuel cells, and for other uses. The characteristics of $La_{1-x}Sr_xMO_{3-\delta}$ are (i) mixed valence state of the 3d transition metals on B sites which results in high electronic conductivity, (ii) large oxygen nonstoichiometry which is related to the high diffusivity of oxide ions, and (iii) formation of solid solutions with a wide miscibility range. In spite of the importance of oxygen nonstoichiometry, limited studies have been made, so far, on the nonstoichiometry and the related defect structure of $La_{1-x}Sr_xMO_{3-\delta}$.

In the previous paper (*1*), the present authors reported the nonstoichiometry of

* To whom correspondence should be addressed.

0022-4596/85 $3.00

$La_{1-x}Sr_xCrO_{3-\delta}$. In the present paper, interest is focused on $La_{1-x}Sr_xFeO_{3-\delta}$. The nonstoichiometry of $LaFeO_{3-\delta}$ is already known to be very small (*2, 3*), while Sr $FeO_{3-\delta}$ shows a large oxygen deficit even at room temperature in air (*4*). At elevated temperatures, $SrFeO_{2.5}$ has been reported. Its structure is brownmillerite in which oxygen vacancies in the perovskite structure are ordered (*4, 5*). The solid solution $La_{1-x}Sr_xFeO_{3-\delta}$ is completely miscible at temperatures above 950°C (*6, 7*).

Mizusaki and his co-investigators have measured the electronic conductivity and Seebeck coefficient for the system La_{1-x} $Sr_xFeO_{3-\delta}$ (x = 0.0, 0.1, and 0.25) as functions of temperature, T, and oxygen partial pressure, P_{O_2}, and have discussed the defect equilibrium in this system (*8, 9*). According to them, the *B*-site Fe ions take mixed valence states: Under oxidizing atmospheres, $Fe^{x}_{Fe}(Fe^{3+})$ and $Fe^{\cdot}_{Fe}(Fe^{4+})$ are predominant, while in reducing atmospheres Fe^{x}_{Fe} and $Fe'_{Fe}(Fe^{2+})$ predominate. [In this paper the Kröger–Vink notation is used (*10*).] The electronic conduction is caused by the exchange of electrons or holes between Fe ions of different valence states. They also interpreted the P_{O_2} dependences of the electronic conductivity and Seebeck coefficient based on the point-defect model of ideal solutions, assuming that the major defects for $LaFeO_{3-\delta}$ are V'''_{La}, $V^{\cdot\cdot}_{O}$, Fe'_{Fe}, and $Fe^{\cdot}_{Fe}$, and those for $La_{1-x}Sr_x$ $FeO_{3-\delta}$ are Sr'_{La}, $V^{\cdot\cdot}_{O}$, Fe'_{Fe}, and $Fe^{\cdot}_{Fe}$. Using this model, they calculated the $V^{\cdot\cdot}_{O}$ concentration, i.e., oxygen nonstoichiometry, as functions of T and P_{O_2}. However, precise measurements on the nonstoichiometry have not yet been made.

The purpose of the present work is to measure the nonstoichiometry, δ, of $La_{1-x}Sr_xFeO_{3-\delta}$ ($0 \leq x \leq 0.6$) as a function of T, P_{O_2}, and *A*-site composition x, and to establish the model of defect equilibrium in this system. The relationship between the results of the present work and those of the conductivity measurements (*8, 9*) will also be discussed.

2. Experimental

2.1. Samples

Samples were prepared by coprecipitation. Aqueous solutions of $La(NO_3)_3$, $Sr(NO_3)_2$, and $Fe(NO_3)_3$ were prepared by dissolving 99.9% reagents of $La_2(CO_3)_3$, $SrCO_3$, and iron ingot, respectively, into HNO_3 aqueous solutions. The concentration of $La(NO_3)_3$ solution was determined by chelate titration using EDTA. The concentrations of two other solutions were determined gravimetrically: The $Sr(NO_3)_2$ solution was poured into a H_2SO_4 solution to precipitate $SrSO_4$. After filtration, the precipitate was baked at 700°C for 12 hr and then weighed in the form of $SrSO_4$. The solution of $Fe(NO_3)_3$ was poured into an NH_4OH solution to form $Fe(OH)_3$. After filtration, the precipitate was also baked at 700°C for 12 hr in air to form Fe_2O_3 and then weighed.

The solutions were mixed together in the proper La : Sr : Fe ratios so that oxide solid solutions with the desired metal ratios would be obtained. Then, the mixtures were poured into an excess of NH_4OH–$(NH_4)_2C_2O_4$ solution to form the coprecipitate of hydroxides and oxalates. After filtration, the coprecipitates were baked at 500 to 800°C, then at 1000°C overnight, and finally at 1300°C for 50 hr. Powder X-ray analysis was employed to confirm formation of the desired perovskite-type solid solution without any trace of a second phase. The $La_{1-x}Sr_xFeO_{3-\delta}$ ($0.1 \leq x \leq 0.6$) powder thus obtained was pressed into rods 5 mm in diameter and 5–20 mm in length, then sintered at 1300°C to prevent pulverization during the measurements, and finally used for thermogravimetry. The $LaFeO_{3-\delta}$ powder was pressed into a rod 5 mm in diameter and 60 mm in length, sintered at 1000°C,

and then converted into a single crystal by means of a floating zone apparatus. The details of the single crystal growth of $LaFeO_{3-\delta}$ are given elsewhere (*11*). A part of the $LaFeO_{3-\delta}$ single crystal was crushed into small pieces and used for thermogravimetric measurements. An other part of the same single crystal was used for measurement of oxide ion diffusion [reported elsewhere (*12*)]. Emission spectrography of the $LaFeO_{3-\delta}$ single crystal showed traces of Si, Mg, Ni, Pb, and Ca as impurities. The concentration of each was well below 0.01%.

2.2. Thermogravimetry

The electric microbalance (Shimazu TG-31H), equipped with a reaction tube and gas circulation and gas mixing systems, was used for thermogravimetry. The sample of 0.5–4 g was placed in an alumina basket which was suspended in the reaction tube from the beam of the electric microbalance. The reaction tube was placed in the electric furnace, the temperature of which was controlled within ±1°C. CO/CO_2 or Ar/O_2 gas mixtures of desired ratios, prepared in the gas mixing system, were introduced into the reaction tube at a total pressure of 0.13 atm and were circulated. The weight change of the sample was recorded by an electric recorder and the equilibrium weight was read precisely by the output voltage of the electric microbalance using a digital voltmeter. The weight of the sample reached a stationary value within 10 min of the introduction of the fresh gas mixture. In order to eliminate the effect of gas composition change in the gas circulation system due to oxidation or reduction of the sample, evacuation of the gas and introduction of a fresh gas mixture of the same ratio were repeated several times until no further weight change could be observed. Corrections were made for buoyancy of the gas so that the weight of the sample under each P_{O_2} and T condition was compared to the calculated weight under 1 atm O_2(g) at 298 K.

According to the preliminary experiments using an alumina rod as a dummy sample, the accuracy of the weight measurement after correction for buoyancy was ±1 μg for each isothermal condition of different gas composition, and ±15 μg for isobaric conditions between room temperature and 1200°C.

Most of the measurements were made at temperatures of 600–1200°C.

3. Results and Discussion

3.1. Thermogravimetry

Typical results of the thermogravimetric measurements are shown in Fig. 1. The relative weight loss $\Delta w/w_0$ is plotted against $\log P_{O_2}$, where w_0 is the weight of each sample in equilibrium with 1 atm O_2(g) at room temperature and Δw is the loss in weight from w_0. The equilibrium weight for each data point was reproducible within ±1 μg. Powder X-ray analysis confirmed that, after thermogravimetry the samples were single phases of the perovskite type. Because the isotherms are continuous, it is evident that the solid solution $La_{1-x}Sr_xFeO_{3-\delta}$ consists of a single phase of the perovskite-type un-

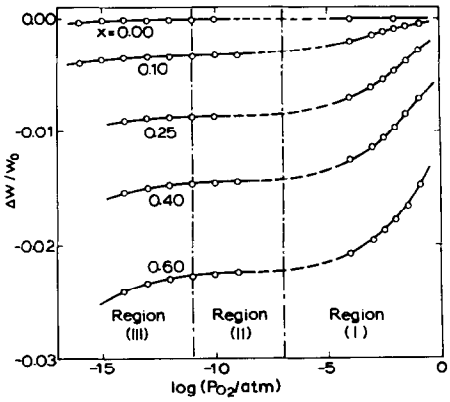

FIG. 1. Relative weight loss, $\Delta w/w_0$, as a function of $\log P_{O_2}$ for $La_{1-x}Sr_xFeO_{3-\delta}$ at 1000°C determined by thermogravimetry.

der the same condition under which our measurements were made.

Apparently, the relation of $\Delta w/w_0$ to log P_{O_2} can be divided into three regions, Regions I–III. In the highest P_{O_2} region (Region I), the weight decreases considerably with decreasing log P_{O_2}. In Region II, the weight is essentially constant, independent of log P_{O_2}. In the lowest log P_{O_2} region (Region III), the weight again decreases with decreasing log P_{O_2}.

3.2. Nonstoichiometry and Defect Equilibrium in $La_{1-x}Sr_xFeO_{3-\delta}$ ($0.1 \leq x \leq 0.6$)

Because analysis of the thermogravimetric data on $LaFeO_{3-\delta}$ is more complicated than that on $La_{1-x}Sr_xFeO_{3-\delta}$ ($0.1 \leq x$), we start from the analysis of the latter.

3.2.1. Nonstoichiometry

From the thermogravimetric data, the relation between δ and log P_{O_2} for $La_{1-x}Sr_xFeO_{3-\delta}$ is calculated (shown by the symbols in Figs. 2 and 3). The solid curves in these figures are calculated based on the defect model described in Sections 3.2.2, 3.2.3, and 3.5.

The point $\delta = 0$ in Figs. 2 and 3 was

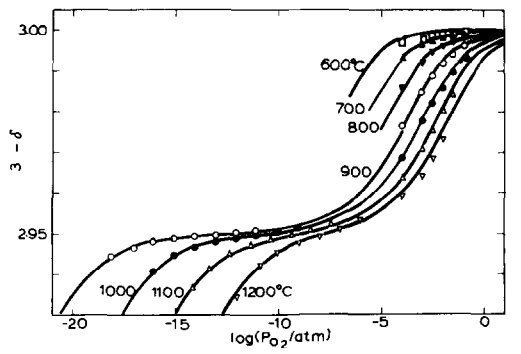

FIG. 2. Nonstoichiometry of $La_{0.9}Sr_{0.1}FeO_{3-\delta}$ in (3 − δ)-vs-log P_{O_2} plots at the temperatures indicated. Symbols show δ values determined by thermogravimetric data. Solid curves are calculated from ΔH°_{ox}, ΔH°_i, ΔS°_{ox}, and ΔS°_i (see Section 3.5).

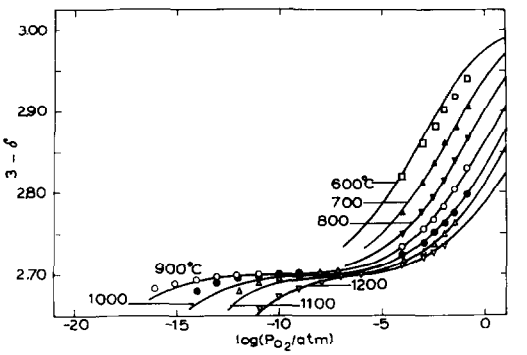

FIG. 3. Nonstoichiometry of $La_{0.75}Sr_{0.25}FeO_{3-\delta}$ in (3 − δ)-vs-log P_{O_2} plots at the temperatures indicated. Symbols show δ values determined by thermogravimetric data. Solid curves are calculated from ΔH°_{ox}, ΔH°_i, ΔS°_{ox}, and ΔS°_i (see Section 3.5).

determined as follows: Previous work on $La_{1-x}Sr_xFeO_{3-\delta}$ (*2–9*) has suggested that this solid solution is oxygen deficient. That is, $\delta \geq 0$ in Regions I–III of Fig. 1. A statistical thermodynamic calculation by Wagner (*13*) showed that $\partial\delta/\partial \log P_{O_2}$ takes the minimum value at the P_{O_2} at which the composition of the sample is stoichiometric. The minimum $\partial w/\partial \log P_{O_2}$ is observed in Region II, indicating that the samples are almost of stoichiometric composition at this point. However, because δ in Region II is considered to be positive, the minimum in Region II cannot correspond to the stoichiometric oxygen content of $\delta = 0$.

It was found that the weight of the sample in any Ar/O_2 or CO/CO_2 gas mixture increases with decreasing temperature. When the sample was cooled in the thermogravimetric apparatus under 0.13 and 1.00 atm of oxygen, the sample increased in weight and then became saturated at about 200°C. The saturated weights for 0.13 and 1.00 atm were the same. These results suggest that the $\partial w/\partial \log P_{O_2}$ value is close to 0 for P_{O_2} values between 0.13 and 1.00 atm below 200°C. Thus, under this condition the weight is considered to correspond to a stoichiometric composition of $\delta = 0$. The estimated error in δ was about 0.0005. This

was due to the error of ± 15 μg in the thermogravimetric measurements.

Using the δ values thus determined, the δ value corresponding to the minimum $\partial\delta/\partial \log P_{O_2}$ in Region II coincides with the value of $x/2$ within $\pm 0.5\%$ for each sample of $La_{1-x}Sr_xFeO_{3-\delta}$ ($0.1 \leq x \leq 0.6$).

3.2.2. Defect Model

According to Mizusaki *et al.* (*9*), the major defects in $La_{1-x}Sr_xFeO_{3-\delta}$ are $V_O^{\cdot\cdot}$, Sr'_{La}, Fe'_{Fe}, and $Fe^{\cdot}_{Fe}$. Under oxidizing atmospheres, the relation $[Fe^{\cdot}_{Fe}] \gg [Fe'_{Fe}]$ holds, while in reducing atmospheres, $[Fe^{\cdot}_{Fe}] \ll [Fe'_{Fe}]$, where [ ] indicates the concentration of each species in number of moles for one mole of $La_{1-x}Sr_xFeO_{3-\delta}$. Based on their model, the δ-vs-log P_{O_2} relations observed in the present work can be interpreted as follows:

The electroneutrality condition for the defects in this solid solution is expressed by

$$[Sr'_{La}] + [Fe'_{Fe}] = 2[V_O^{\cdot\cdot}] + [Fe^{\cdot}_{Fe}]. \quad (1)$$

The value of $[Sr'_{La}]$ is given by the nominal A-site composition x. That is,

$$[Sr'_{La}] = x. \quad (2)$$

Because this solid solution is an oxygen deficient type, we have

$$[V_O^{\cdot\cdot}] = \delta. \quad (3)$$

From Eqs. (1)–(3), we have

$$x + [Fe'_{Fe}] = 2\delta + [Fe^{\cdot}_{Fe}]. \quad (4)$$

In an oxidizing atmosphere, Eq. (4) can be simplified to

$$x \simeq 2\delta + [Fe^{\cdot}_{Fe}]. \quad (4a)$$

With decreasing P_{O_2}, $[Fe^{\cdot}_{Fe}]$ becomes sufficiently low so that

$$x \simeq 2\delta. \quad (4b)$$

In a reducing atmosphere, Eq. (4) can be simplified to

$$x + [Fe'_{Fe}] \simeq 2\delta. \quad (4c)$$

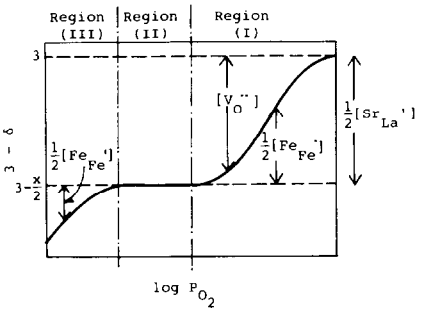

FIG. 4. A schematic diagram for the concentrations of the defects $[Sr'_{La}]$, $[V_O^{\cdot\cdot}]$, $[Fe'_{Fe}]$, and $[Fe^{\cdot}_{Fe}]$ as functions of log P_{O_2} for $La_{1-x}Sr_xFeO_{3-\delta}$.

Figure 4 is a schematic diagram of the defect concentrations as a function of log P_{O_2}. The plateau in Region II corresponds to $\delta \simeq x/2$. At the minimum $\partial\delta/\partial \log P_{O_2}$ in Region II, the "stoichiometric" composition holds for the electronic defects, i.e., $[Fe^{\cdot}_{Fe}] = [Fe'_{Fe}]$. In Region I, the electroneutrality condition is expressed by Eq. (4a), while that for Region III is given by Eq. 4c.

3.2.3. Defect Equilibrium

The reaction between oxygen gas and the defects in $La_{1-x}Sr_xFeO_{3-\delta}$ can be expressed as

$$\tfrac{1}{2}O_2(g) + V_O^{\cdot\cdot} + 2Fe^{x}_{Fe} = O^{x}_{O} + 2Fe^{\cdot}_{Fe}. \quad (5)$$

The equilibrium condition for the reaction is

$$K_{ox} = \frac{[O^{x}_{O}][Fe^{\cdot}_{Fe}]^2}{P_{O_2}^{1/2}[V_O^{\cdot\cdot}][Fe^{x}_{Fe}]^2} = \frac{(3-\delta)[Fe^{\cdot}_{Fe}]^2}{P_{O_2}^{1/2}\delta[Fe^{x}_{Fe}]^2} \quad (6)$$

where K_{ox} is the equilibrium constant. The Fe^{3+} ions (Fe^{x}_{Fe}) are expected to experience disproportionation into Fe^{2+}(Fe'_{Fe}) and Fe^{4+}($Fe^{\cdot}_{Fe}$). That is,

$$2Fe^{x}_{Fe} = Fe'_{Fe} + Fe^{\cdot}_{Fe}. \quad (7)$$

The equilibrium constant is given by

$$K_i = \frac{[Fe^{\cdot}_{Fe}][Fe'_{Fe}]}{[Fe^{x}_{Fe}]^2}. \quad (8)$$

The number of moles of Fe in $La_{1-x}Sr_x$

$FeO_{3-\delta}$ is unity. Therefore, we obtain the relation

$$[Fe^{x}_{Fe}] + [Fe^{\cdot}_{Fe}] + [Fe^{\prime}_{Fe}] = 1. \quad (9)$$

Combining Eqs. (2)–(4), (6), (8), and (9), we can eliminate the terms $[Fe^{\prime}_{Fe}]$, $[Fe^{\cdot}_{Fe}]$, and $[Fe^{x}_{Fe}]$ from these equations to obtain the relation

$$\frac{(2\delta - x + 1)\delta^{1/2}P_{O_2}^{1/4}}{(2\delta - x)(3 - \delta)^{1/2}} = \frac{K_i}{K_{ox}} \frac{(3 - \delta)^{1/2}(x + 1 - 2\delta)}{(2\delta - x)^{1/2}P_{O_2}^{1/4}} - k_{ox}^{-1/2}. \quad (10)$$

When we put

$$Y = \frac{(2\delta - x + 1)\delta^{1/2}P_{O_2}^{1/4}}{(2\delta - x)(3 - \delta)^{1/2}}, \quad (11)$$

$$X = \frac{(3 - \delta)^{1/2}(x - 1 + 2\delta)}{(2\delta - x)^{1/2}P_{O_2}^{1/4}}, \quad (12)$$

$$A = K_i/K_{ox}, \quad (13)$$

and

$$B = -K_{ox}^{-1/2}, \quad (14)$$

Eq. (10) can be expressed by

$$Y = AX + B. \quad (15)$$

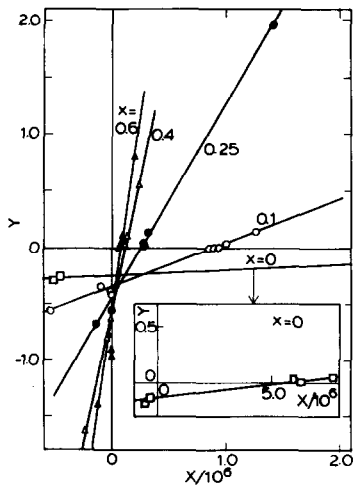

FIG. 5. Plots of Y vs X for the determination of K_{ox} and K_i for $La_{1-x}Sr_xFeO_{3-\delta}$ of different x.

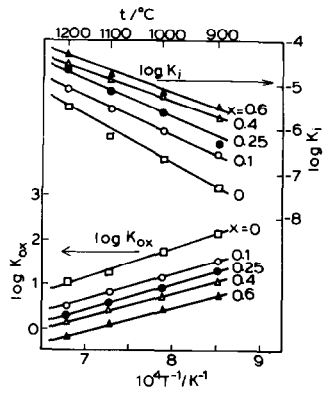

FIG. 6. Van't Hoff plots for K_{ox} and K_i of $La_{1-x}Sr_xFeO_{3-\delta}$ of different x.

The values of X and Y were calculated from the observed (δ, P_{O_2}) values. Typical relations of Y to X are shown in Fig. 5. They are linear, and from the slope and intercept of the plots, the constants A and B are calculated. From A and B, K_i and K_{ox} are determined and are shown as the van't Hoff plot in Fig. 6.

3.3. Nonstoichiometry and Defect Equilibrium in $LaFeO_{3-\delta}$

3.3.1. Nonstoichiometry and Defect Model

Figure 7 shows the log δ-vs-log P_{O_2} plot for $LaFeO_{3-\delta}$, where the symbols without parentheses indicate the δ values calculated from the observed weight changes assuming that δ in $LaFeO_{3-\delta}$ is zero below 200°C under 1 atm P_{O_2}.

The minimum $\partial\delta/\partial \log P_{O_2}$ in Region II is observed at $\delta = 0.0015$. If this plateau is caused by divalent cationic impurities, x in $LaFeO_{3-\delta}$ should be 0.003. This value seems too high because the analyzed impurity concentrations amount to well below 0.05% (or 0.0005).

From electronic conductivity and Seebeck coefficient results for $LaFeO_{3-\delta}$, Mizusaki *et al.* (*8*) concluded that the La $FeO_{3-\delta}$ prepared by them had La vacancies

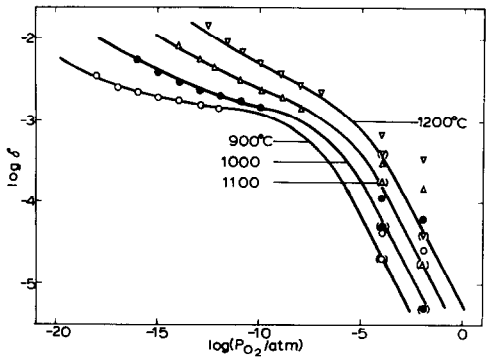

FIG. 7. Nonstoichiometry of $LaFeO_{3-\delta}$ in log δ-vs-log P_{O_2} plots at the temperatures indicated. Symbols show δ values determined by thermogravimetric data. Symbols in parentheses indicate δ_R, the δ values corrected based on the defect model described in Section 3.3.2. Solid curves are calculated from ΔH°_{ox}, ΔH°_i, ΔS°_{ox}, and ΔS°_i (see Section 3.5.).

due to a nonstoichiometric La/Fe ratio. The $[V'''_{La}]$ was estimated to be 0.0007. Since V'''_{La} is trivalent, the charge-balance consideration gives the effective x value due to $[V'''_{La}]$ as

$$x = 3[V'''_{La}]. \quad (16)$$

Thus, for their sample, $x = 0.0021$ was obtained. This value is close to 0.003, which was observed in the present work.

There are differences in the starting materials and in the preparation procedure between the $LaFeO_{3-\delta}$ used in this work and that used previously (*8*): In this work, the sample was a single crystal grown by the floating zone apparatus, while in the previous work, the samples were sintered at 1600°C. In spite of these differences, the values corresponding to x are close to each other. Therefore, it is concluded that the source of the nonstoichiometry term, x, is not the impurity cations but the intrinsic defects in $LaFeO_{3-\delta}$. It is difficult to prepare a sample in which the La/Fe ratio is exactly unity. Therefore, although X-ray analysis did not show the existence of a second phase, it is probable that the sample, as prepared, contained a trace amount of La_2O_3 or iron oxides. The deviation of the La/Fe ratio from stoichiometry for $LaFeO_{3-\delta}$ coexisting with La_2O_3 may be different from that for $LaFeO_{3-\delta}$ coexisting with iron oxides. In the former $LaFeO_{3-\delta}$ a deficiency in Fe is expected, while in the latter, a deficiency in La may exist.

It is known that the sintered $LaFeO_{3-\delta}$ sample containing a slight amount of La_2O_3 tends to break down into powder because La_2O_3 is hygroscopic. Such a phenomenon has not been observed in the present work. Thus, it is probable that the $LaFeO_{3-\delta}$ samples in this work had a slight excess of iron oxide and, consequently, V'''_{La} was formed. The molar ratio of $Fe_2O_3/LaFeO_{3-\delta}$ in the sample was estimated to be less than 0.001 because no significant discontinuity was observed on the $\Delta w/w_0$-vs-log P_{O_2} plots due to the phase changes $Fe_2O_3 \rightleftarrows Fe_3O_4 \rightleftarrows FeO$. The concentration of V'''_{La} may have been fixed by the equilibrium between iron oxides and $LaFeO_{3-\delta}$ at the highest temperature at which the samples were treated, i.e., at the melting point of $LaFeO_{3-\delta}$ in this work and at 1600°C in Ref. (*8*).

The defects assumed in $LaFeO_{3-\delta}$ are V'''_{La}, $Fe^{\cdot}_{Fe}$, Fe'_{Fe}, and $V^{\cdot\cdot}_{O}$. Using x defined by Eq. (16), the electroneutrality condition in $LaFeO_{3-\delta}$ can be expressed by Eq. (4).

3.3.2. Reevaluation of Nonstoichiometry and Calculation of Defect Equilibrium Constants

The method described in Section 3.2.3 can be applied to the calculation of K_i and K_{ox} for $LaFeO_{3-\delta}$. Using $x = 0.003$ and the observed δ-vs-P_{O_2} relation, we have determined the preliminary K_i and K_{ox} values. Then, using Eqs. (4), (6), (8), and (9) and the preliminary K_i and K_{ox} values, the relation of δ to P_{O_2} has been recalculated. The results of these preliminary calculations leads to the relationship $\delta \propto P_{O_2}^{-1/2}$ for the region of P_{O_2} (atm) $> 10^{-5}$, independent of temperature. The $P_{O_2}^{-1/2}$ dependence of δ is consistent with the results of the electronic

conductivity (*8*) and isotopic diffusion coefficient of oxide ions (*12*). However, the observed results (shown in Fig. 7) indicate that δ depends on $P_{O_2}^{-1/3}$ to $P_{O_2}^{-1/5}$. This difference may be due to the experimental error of ± 0.0005 in δ. It is serious particularly for $\log(P_{O_2}/\text{atm}) > -4$, in which region δ values are less than 0.001.

The nonstoichiometric data for $LaFeO_{3-\delta}$ were reevaluated as follows. When we assume that δ depends on $P_{O_2}^{-1/2}$ above 10^{-4} atm P_{O_2}, the observed δ values can be related to the real δ values, δ_R, by the equation

$$\delta - \delta_0 = \delta_R = AP_{O_2}^{-1/2}, \qquad (17)$$

where δ_0 and A are constants. For each temperature, δ_0 and A were calculated from the observed δ and P_{O_2} values. They are shown in Table I. In Fig. 7, the δ_R values calculated by Eq. (17) are indicated by the symbols in parentheses. For $P_{O_2}/\text{atm} < 10^{-4}$, δ_R values were essentially identical to δ values. The K_i and K_{ox} values for $La FeO_{3-\delta}$ were calculated using the corrected δ values and Eqs. (10)–(15). The plot of Y vs X is shown in the inset to Fig. 5. The K_i and K_{ox} values are shown in Fig. 6.

3.4. Relationship among K_i, K_{ox}, Temperature, and Composition

As shown in Fig. 6, $\log K_i$ and $\log K_{ox}$ depend linearly on $1/T$. When we express the standard Gibbs free energy change, the standard enthalpy change, and the standard entropy change for the reaction of Eq. (5) as ΔG°_{ox}, ΔH°_{ox}, and ΔS°_{ox}, respectively, we have the relationship

$$-RT \ln K_{ox} = \Delta G^\circ_{ox} = \Delta H^\circ_{ox} - T\Delta S^\circ_{ox}. \qquad (18)$$

Similarly, K_i is related to the standard Gibbs free energy change ΔG°_i, enthalpy change ΔH°_i, and entropy change ΔS°_i of the reaction of Eq. (7) by

$$-RT \ln K_i = \Delta G^\circ_i = \Delta H^\circ_i - T\Delta S^\circ_i. \qquad (19)$$

The ΔH°_{ox}, ΔS°_{ox}, ΔH°_i, and ΔS°_i values for each composition x are calculated by the least-squares method and are shown in Figs. 8 and 9. Empirically, these values depend linearly on x, including those for $La FeO_{3-\delta}$ in which δ is very small compared to δ for other compositions.

TABLE I

CORRELATION OF δ FOR $LaFeO_{3-\delta}$

t(°C)	δ_0	A
900	2.41×10^{-5}	1.97×10^{-7}
1000	5.59×10^{-5}	4.79×10^{-7}
1100	1.22×10^{-4}	1.64×10^{-6}
1200	2.86×10^{-4}	3.46×10^{-6}

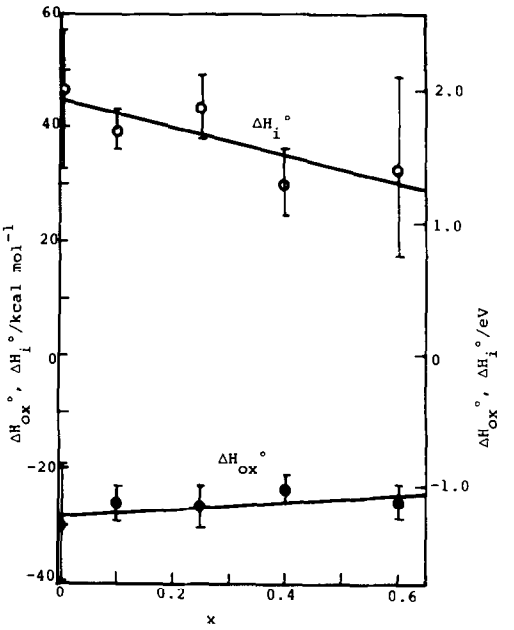

FIG. 8. Plots of ΔH°_{ox} and ΔH°_i as functions of x of $La_{1-x}Sr_xFeO_{3-\delta}$. Error bars show the 2σ values.

3.5. Defect Concentration Diagrams

Using ΔH°_{ox}, ΔS°_{ox}, ΔH°_i, and ΔS°_i given by the linear relationships in Figs. 8 and 9, we can calculate the defect concentrations in $La_{1-x}Sr_xFeO_{3-\delta}$ of any x value under any P_{O_2} and T condition by Eqs. (4), (6), (8), (9),

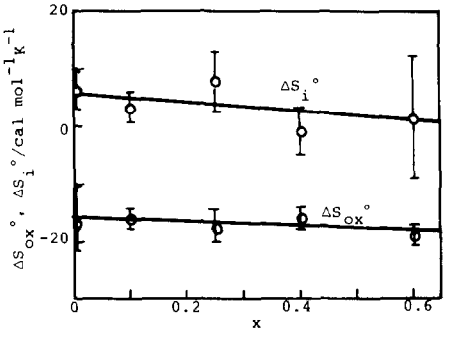

FIG. 9. Plots of ΔS_{ox}° and ΔS_i° as functions of x of $La_{1-x}Sr_xFeO_{3-\delta}$. Error bars show 2σ values.

(18), and (19). The solid curves in Figs. 2, 3, and 7 are recalculated δ (= $[V_O^{\cdot\cdot}]$) values. By the agreement between the observed δ-vs-log P_{O_2} relationship and the recalculated one, it is confirmed that the K_i and K_{ox} values are constant independent of δ in spite of the large δ value in $La_{1-x}Sr_xFeO_{3-\delta}$. Figure 10 shows the calculated defect concentrations for $La_{0.6}Sr_{0.4}FeO_{3-\delta}$ as functions of log P_{O_2}. Figure 11 shows them at 1000 and 1200°C in air as functions of x. At this condition, partial replacement of La by Sr effects the formation of both $V_O^{\cdot\cdot}$ and $Fe_{Fe}^{\cdot}$. However, for $x \geq 0.4$, $[Fe_{Fe}^{\cdot}]$ tends to decrease with increasing x.

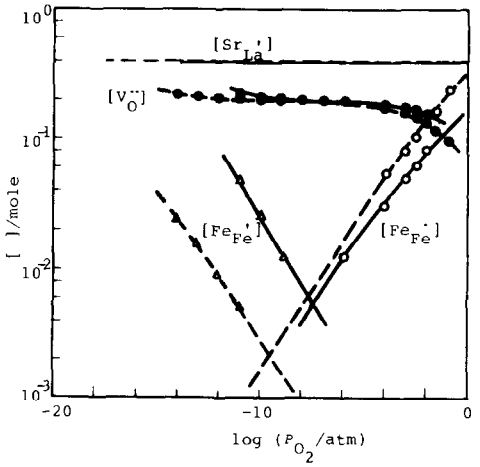

FIG. 10. Defect concentrations as a function of log P_{O_2} for $La_{0.6}Sr_{0.4}FeO_{3-\delta}$. ---, 1000°C; —, 1200°C.

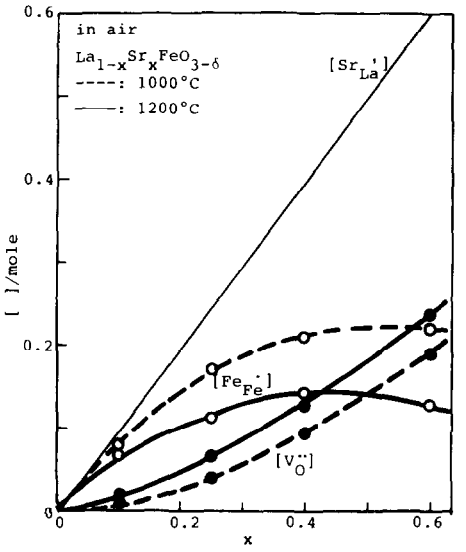

FIG. 11. Defect concentrations as a function of x of $La_{1-x}Sr_xFeO_{3-\delta}$ in air. ---, 1000°C; —, 1200°C.

3.6. Pseudo-bandgap of $La_{1-x}Sr_xFeO_{3-\delta}$

Because the carriers in $La_{1-x}Sr_xFeO_{3-\delta}$ are Fe_{Fe}' and $Fe_{Fe}^{\cdot}$, ΔH_i°, the enthalpy change for the reaction $2Fe_{Fe}^{x} = Fe_{Fe}' + Fe_{Fe}^{\cdot}$, can be considered a pseudo-bandgap. Mizusaki *et al.* (*9*) have determined the ΔH_i° values for $LaFeO_{3-\delta}$, $La_{0.9}Sr_{0.1}FeO_{3-\delta}$, and $La_{0.75}Sr_{0.25}FeO_{3-\delta}$ from the Seebeck coefficient and electronic conductivity measurements. Their results are listed in Table II along with those of the present work. The former values are larger than the latter ones by 0.2–0.4 eV.

In Ref. (*9*), the ΔH_i° values were calcu-

TABLE II

COMPARISON OF ΔH_i° VALUES

	ΔH_i° (eV)	
	This work	Ref. (*9*)
$LaFeO_{3-\delta}$	1.9	2.3
$La_{0.9}Sr_{0.1}FeO_{3-\delta}$	1.8	2.0
$La_{0.75}Sr_{0.25}FeO_{3-\delta}$	1.65	2.0

lated assuming that the activation energies for the hopping of electrons (the electron exchange between Fe'_{Fe} and Fe^{x}_{Fe}) and holes (the electron exchange between Fe^{x}_{Fe} and $Fe^{\cdot}_{Fe}$) were zero. However, in the same paper, they also suggested that the activation energies for hopping would be 0.15 ± 0.10 eV for holes and 0.05 ± 0.10 eV for electrons.

The ΔH_i° values in Ref. (*9*) are considered to include the sum of the hopping energies of holes and electrons. According to their estimation, the sum is 0.20 ± 0.20 eV. This value is close to the difference in ΔH_i° between the two works. It is concluded that the pseudo-bandgap for $La_{1-x}Sr_xFeO_{3-\delta}$ is given by the ΔH_i° values determined in this work. The hopping energies for holes and electrons are probably about 0.15 and 0.05 eV, respectively, as stated in the preceding work (*9*).

4. Conclusion

The nonstoichiometry in $La_{1-x}Sr_xFeO_{3-\delta}$ ($0.1 \leq x \leq 0.6$) was found to be very large while that in $LaFeO_{3-\delta}$ was small. Major defects in $La_{1-x}Sr_xFeO_{3-\delta}$ ($0.1 \leq x$) were found to be Sr'_{La}, $V_O^{\cdot\cdot}$, Fe'_{Fe}, and $Fe^{\cdot}_{Fe}$. In spite of the large nonstoichiometry, the equilibrium constants of the defects and surrounding oxygen atmosphere were determined independent of the δ value. For $LaFeO_{3-\delta}$ and, maybe, $La_{1-x}Sr_xFeO_{3-\delta}$ of very small x, cation defects due to the nonstoichiometric (La + Sr)/Fe ratio also affect the defect equilibrium. However, the defect equilibrium constants in $LaFeO_{3-\delta}$ are found to be essentially identical to those in $La_{1-x}Sr_xFeO_{3-\delta}$ ($0.1 \leq x$), with a monotonous dependence with Sr content.

References

1. J. MIZUSAKI, S. YAMAUCHI, K. FUEKI, AND A. ISHIKAWA, *Solid State Ionics* **12,** 119 (1984).
2. T. NAKAMURA, G. PETZOW, AND L. J. GAUCKLER, *Mater. Res. Bull.* **14,** 649 (1979).
3. U. SHIMONY AND J. M. KNUDSEN, *Phys. Rev.* **114,** 761 (1966).
4. J. B. MACCHESNEY, R. C. SHERWOOD, AND J. F. POTTER, *J. Chem. Phys.* **43,** 1907 (1965).
5. P. K. GALLAGHER, J. B. MACCHESNEY, AND D. N. E. BUCHANAN, *J. Chem. Phys.* **41,** 2429 (1964).
6. H. YAMAMURA AND R. KIRIYAMA, *Nippon Kagaku Kaishi,* 343 (1972).
7. T. SASAMOTO, J. MIZUSAKI, M. YOSHIMURA, W. R. CANNON, AND H. K. BOWEN, *Yogyo-Kyokai-Shi* **90,** 24 (1982).
8. J. MIZUSAKI, T. SASAMOTO, W. R. CANNON, AND H. K. BOWEN, *J. Amer. Ceram. Soc.* **65,** 363 (1982).
9. J. MIZUSAKI, T. SASAMOTO, W. R. CANNON, AND H. K. BOWEN, *J. Amer. Ceram. Soc.* **66,** 247 (1983).
10. F. A. KRÖGER, "The Chemistry of Imperfect Crystals," Vol. 1–3, North-Holland, Amsterdam (1974).
11. T. MATSUURA, T. ISHIGAKI, J. MIZUSAKI, S. YAMAUCHI, AND K. FUEKI, *Japan. J. Appl. Phys. Part 1* **23,** 1172 (1984).
12. T. ISHIGAKI, S. YAMAUCHI, J. MIZUSAKI, K. FUEKI, H. NAITO, AND T. ADACHI, *J. Solid State Chem.* **55,** 50 (1984).
13. C. WAGNER, *Prog. Solid State Chem.* **6,** 1 (1971).